

# Classical Many-particle Clusters in Two Dimensions

G. Date\*, M. V. N. Murthy<sup>†</sup> and Radhika Vathsan<sup>‡</sup>  
*The Institute of Mathematical Sciences, Madras 600 113, India.*

(October 11, 2018)

## Abstract

We report on a study of a classical, finite system of confined particles in two dimensions with a two-body repulsive interaction. We first develop a simple analytical method to obtain equilibrium configurations and energies for few particles. When the confinement is harmonic, we prove that the first transition from a single shell occurs when the number of particles changes from five to six. The shell structure in the case of an arbitrary number of particles is shown to be independent of the strength of the interaction but dependent only on its functional form. It is also independent of the magnetic field strength when included. We further study the effect of the functional form of the confinement potential on the shell structure. Finally, we report some interesting results when a three-body interaction is included, albeit in a particular model.

PACS numbers: 02.60.Cb, 71.10.-w

Typeset using REVTeX

---

\*email: shyam@imsc.ernet.in

†email: murthy@imsc.ernet.in

‡email: radhika@imsc.ernet.in

## I. INTRODUCTION

Two dimensional clusters or “artificial atoms” have attracted considerable attention in recent years [1]. A cluster of a finite number of charged particles confined by an external potential may be regarded as an “artificial atom”. There are several examples of such systems from mesoscopic systems to the astrophysical system. In observed systems such as electrons on a liquid helium film [2], drops of colloidal suspensions [3] and confined dusty particles [4], the dynamics is essentially classical. On the other hand, in mesoscopic systems like quantum dots, quantum effects may not be negligible [5]. The actual Hamiltonians which capture the full dynamics of these systems are rather complicated. However, several studies assuming model systems have been carried out. In particular, there have been studies on the ordering and transitions of charged particles in two dimensions [6–10].

In a recent Monte Carlo study, Bedanov and Peeters [9] (see also Bolten and Rossler [10]) have analysed the classical ground state of a system of confined, charged particles interacting through the Coulomb interaction. By minimising the classical energy, they obtain numerically the shell structure in a cluster of  $N$  particles. They have systematically listed the shell structure in a “Mendeleev” table for  $N \leq 52$ , and for a few large clusters. Similar results are available also for logarithmic two-body interaction [6]. An important fact that follows from this Mendeleev table is that the charged particles, confined in a parabolic potential, arrange themselves in concentric shells where each shell may be thought of as an annulus whose width is much smaller than the radius. For particular numbers,  $N = 6, 19, 37, \dots$  these annuli are almost precisely circles. These are called magic numbers. There are further systematics (approximate) in this table. Up to  $N = 5$ , the particles in the ground state configuration arrange themselves on a circle. For  $N = 6$ , there are five particles on the circle and one in the centre (circle-dot) in the ground state. With the addition of more particles, a second shell starts forming until the arrangement has 5 particles in the inner shell and 10 particles on the outer shell, ie  $N = 15$ . Addition of one more particle ( $N = 16$ ), creates a configuration similar to  $N = 15$  with the extra particle at the centre. It is interesting to note that the multi-shell structure was *experimentally* observed by Christian Myer [11] more than a hundred years ago. He observed these geometric transitions in a system involving magnetic needles floating on water, confined by a bar magnet held above the surface. The result, as quoted by J. J. Thompson, notes that five magnetic needles always remained on the circumference of a circle whereas the sixth one, when added, always drifted to the middle. Notice that the interaction between magnetic needles is different from Coulomb interaction. Nevertheless the observed phenomenon bears resemblance to the numerical results.

At least up to  $N = 50$ , the geometric transition from 5 to 6, that is from a circle to a circle-dot, forms a template for the innermost shell. To a very good approximation, the number of shells for any  $N$ , in the Mendeleev table [9], may be deduced as follows: Write a given  $N$  as a sum of non-repeating multiples of five and a remainder. The number of terms in the sum is the number of shells. For example,  $N = 48$  may be written as  $N = 5 + 10 + 15 + 13$ . This, in our way of looking, corresponds to having four shells. (It is not expected that this will hold for large  $N$  since the system goes into a hexagonal arrangement in the bulk.) The main theme of the paper is this geometric transition from circle to circle-dot configuration when the number of particles changes from 5 to 6. We also derive some general results concerning the shell-structure for arbitrary  $N$ .

In this paper we first consider a cluster of  $N$  particles in which the repulsive two-body potential is a power-law. The classical system we are interested in, to begin with, consists of  $N$  particles of equal mass  $m$ , confined in an oscillator potential, in a uniform magnetic field and interacting via a two-body potential. The Hamiltonian of such a system of particles is given by

$$H = \sum_{i=1}^N \left[ \frac{(\vec{p}_i + \vec{a}_i)^2}{2m} + \frac{1}{2} m \omega^2 r_i^2 \right] + \beta \sum_{i,j(j \neq i)} \frac{1}{(r_{ij}^2)^\nu}, \quad (1)$$

where  $\vec{r}_i$  and  $\vec{p}_i$  denote the position and momentum vectors of the particle with index  $i$ . The vector potential, for a uniform magnetic field in the symmetric gauge, is given by

$$(a_i)_x = -\omega_L y_i \quad ; \quad (a_i)_y = \omega_L x_i, \quad (2)$$

where  $\omega_L$  is the Larmor frequency and  $\vec{r}_{ij} = \vec{r}_i - \vec{r}_j$ . The power  $\nu$  (positive) is kept arbitrary. The Coulomb Hamiltonian is recovered by choosing  $\nu = 1/2$ . We also consider the case when the two-body interaction is of the form  $-\beta \sum_{i,j(j \neq i)} \log(r_{ij}^2/\rho^2)$  which is repulsive for  $r_{ij}^2 < \rho^2$  (see Appendix A). This may be closer to the real situation as also the  $\nu = 1/2$  (Coulomb) case for electrons in a quantum dot [12]. Recently, the  $\nu = 1$  (inverse square interaction) case has also been analysed in detail [13] because of its relevance to quantum dot systems. In addition, this case nicely lends itself to analytical manipulations.

We devise a simple analytical method to obtain the classical ground state energy in *two* steps. First, we extremise the energy for a *fixed* total angular momentum  $J$  (which is conserved), and then minimise this energy with respect to  $J$ . This has two advantages. It reflects the quantum degeneracy of the lowest Landau level for electrons in a uniform magnetic field in the absence of any interaction, at the classical level itself and secondly it allows one to do the second step of the minimisation over the quantised values of the angular momentum. Here, however, we restrict ourselves to a classical analysis only and derive some exact results analytically for the equilibrium configurations.

In Section II, we show that:

1. The configurations extremising the energy, modulo overall scale, are *independent* of the parameters of the Hamiltonian and also of the angular momentum  $J$  so long as the repulsive two-body potential falls off as a power-law with the relative distance and the confinement is harmonic. Only the overall length scale is sensitive to these details.
2. Two special configurations, one in which all the  $N$  particles are on a circle (referred to as  $\bigcirc$ ) and the one in which  $N - 1$  are on a circle with one at the center (referred to as  $\odot$ ) are always equilibrium configurations. We give exact analytical expressions for the corresponding energy for all  $N$  and  $\nu$ . The  $\bigcirc$  has lower energy for  $N \leq 5$  while  $\odot$  has lower energy for  $N \geq 6$ . In fact the  $\bigcirc$  is the ground state for all  $N \leq 5$  while  $\odot$  is the ground state for  $N = 6, 7, 8$ . (This is a well known result for Coulomb interaction [10,9] but is also true in the general case considered below for arbitrary  $\nu$  up to a maximum value which depends on the number of particles.) This geometric transition in the ground state is the first one to occur and is *independent* of the precise form of the repulsive interaction.

3. While it is known *numerically* that for  $N \geq 9$  and for Coulomb potential [9,10] the minimum energy configurations exhibit approximate multi-shell structure, the special configurations provide an upper bound on the minimum energy for a whole class of interactions that we consider here. The results presented in this section are an elaboration of our previous work [14].

In Section III, we consider the effect of confinement on the geometric transition which occurs for  $N$  from 5 to 6. The one-body confinement in eq.(1) is generalised to  $V_{conf} = \sum_{i=1}^N (r_i^2)^\gamma$ . The oscillator confinement is recovered for  $\gamma = 1$ . Surprisingly, we find that there exists a critical value of  $\nu$  above which the first geometric transition always occurs between 5 and 6 for  $\gamma > 1$  and between 4 and 5 for  $\gamma < 1$ .

In Section IV, we consider the effect of three-body perturbations on this geometric transition. We do so by using a particular model Hamiltonian whose exact quantum mechanical ground state energy and wave function are known in a limit to be defined later. While this again has interesting properties in its own right, it is included here primarily to study its effect on shell formation. Some of questions relating to three-body perturbations are being studied and will be published else where [20].

We conclude in Section V with some comments and future prospects. Appendix A contains some general results concerning the logarithmic interaction potential. Details of our numerical simulations are discussed in Appendix B. These are used to check our results with ref. [9] for the case of Coulomb potential and then extended to other forms of the potential.

## II. GEOMETRY OF CLUSTERS IN PARABOLIC CONFINEMENT

In this section we consider the classical equilibrium configurations of the Hamiltonian given by eq.(1). The Hamiltonian can be written in terms of dimensionless units by introducing a length scale  $l = \sqrt{\hbar/(m\omega)}$  which is the basic oscillator length. All distances are measured in terms of this basic length unit. Note that  $\hbar$  is introduced only as a convenience so that the energy is measured in units of  $\hbar\omega$  and does not have any other significance as in the quantum case. The analysis presented in this paper is entirely classical. The momenta are measured in units of  $\hbar/l$ .

The new Hamiltonian in these scaled units, but keeping the same notation, may be written as

$$\frac{H}{\hbar\omega} = \sum_{i=1}^N \left[ \frac{\vec{p}_i^2}{2} + \frac{1}{2}(1 + \alpha^2)r_i^2 + \alpha j_i \right] + g \sum_{i,j(j \neq i)} \frac{1}{(r_{ij}^2)^\nu}, \quad (3)$$

where  $j_i = x_i p_{iy} - y_i p_{ix}$ ,  $\alpha = \frac{\omega_L}{\omega}$  and  $g = \frac{\beta}{\hbar\omega} (l)^{2\nu}$ . Unless otherwise mentioned the summations run from 1 to  $N$  hereafter. While the original coupling constant  $\beta$  was dimensional the new coupling constant  $g$  is dimensionless. Hereafter we assume all the energies are measured in units of  $\hbar\omega$  and do not write the units explicitly.

To find the equilibrium configurations we carry out the variation in two steps. For the first step of the variation we introduce the function

$$F = H + \lambda \left( \sum_i j_i - J \right), \quad (4)$$

where  $j_i$  are the single particle angular momenta and  $\lambda$  is the Lagrange multiplier which enforces the constraint  $J = \sum_i j_i$ . Setting  $\delta F = 0$ , where the variation is done in the full phase space variables, gives the necessary equations to determine the equilibrium configuration in the phase space,

$$p_{ix} = (\alpha + \lambda)y_i, \quad (5)$$

$$p_{iy} = -(\alpha + \lambda)x_i, \quad (6)$$

$$(1 - \lambda^2 - 2\alpha\lambda)\vec{r}_i = 4g\nu \sum_{j(j \neq i)} \frac{\vec{r}_{ij}}{(r_{ij}^2)^{\nu+1}}. \quad (7)$$

This is the basic set of equations. Any solution to this set of equations describes an equilibrium configuration which could be a local minimum/maximum or a saddle point. We also remark that while the Hamiltonian is written in a particular symmetric gauge, the variational equations given above are actually gauge invariant. The main advantage of introducing  $F$  instead of  $H$  for variation is that it allows us to keep the dependence of the variational equations on the magnetic field even at the classical level. If we vary  $H$  separately this advantage is lost. We may also include the case of logarithmic interaction by simply setting the power  $\nu = 0$  and by setting the prefactor to  $4g$  instead of  $4g\nu$  in eq.(7). To avoid confusion, however, we briefly discuss the results for the logarithmic case separately in Appendix A.

First we present a qualitative but general analysis of this basic set of equations without making any assumptions. To make the analysis simple, we introduce an auxiliary variable,

$$\phi = \sum_i r_i^2. \quad (8)$$

The total angular momentum may now be written in terms of this auxiliary variable as

$$J = \sum_i (x_i p_{iy} - y_i p_{ix}) = -(\alpha + \lambda)\phi, \quad (9)$$

where we have made use of eqs.(5,6). It is convenient to express  $\vec{r}_i = R\vec{s}_i$  where  $R$  is a common scale factor which may be taken to be the radius of the farthest particle, say the  $N^{th}$  one, and  $\vec{s}_i$  denotes the internal variables. Therefore

$$\phi = R^2 \left[ \sum_{i=1}^{N-1} s_i^2 + 1 \right] \equiv R^2 \tilde{\phi} \quad (10)$$

since  $s_N^2 = 1$  by choice. Using eq.(7) and eliminating  $\lambda$ -dependence using eq.(9), we have

$$\frac{(R^2)^{\nu+1}}{4g\nu} \left[ 1 + \alpha^2 - \frac{J^2}{R^4 \tilde{\phi}^2} \right] \vec{s}_i = \sum_{j(j \neq i)} \frac{\vec{s}_{ij}}{(s_{ij}^2)^{\nu+1}}. \quad (11)$$

Taking the scalar product with  $\vec{s}_i$  and dividing both sides by  $s_i^2$  ( $\neq 0$ ), we get

$$\frac{(R^2)^{\nu+1}}{4g\nu} \left[ 1 + \alpha^2 - \frac{J^2}{R^4 \tilde{\phi}^2} \right] = \sum_{j(j \neq i)} \frac{1 - (s_j/s_i) \cos(\theta_{ij})}{(s_i^2 + s_j^2 - 2s_i s_j \cos(\theta_{ij}))^{\nu+1}}. \quad (12)$$

Note that the LHS is independent of the particle index  $i$ . Thus we have  $N - 1$  independent of equations of the type

$$\sum_{j(j \neq i)} \frac{1 - (s_j/s_i) \cos(\theta_{ij})}{(s_i^2 + s_j^2 - 2s_i s_j \cos(\theta_{ij}))^{\nu+1}} = \sum_{j(j \neq k)} \frac{1 - (s_j/s_k) \cos(\theta_{kj})}{(s_k^2 + s_j^2 - 2s_k s_j \cos(\theta_{kj}))^{\nu+1}}, \quad \forall \quad k \neq i. \quad (13)$$

Further by taking the cross product with  $\vec{s}_i$  and dividing by  $s_i$ , we get,

$$\sum_{j(j \neq i)} \frac{s_j \sin(\theta_{ij})}{(s_i^2 + s_j^2 - 2s_i s_j \cos(\theta_{ij}))^{\nu+1}} = 0, \quad (14)$$

which provides a further set of  $N$  conditions on the internal coordinates  $\vec{s}_i$ . Notice that these conditions are manifestly scale invariant. Together, eqs.(13,14) provide the  $2N - 1$  necessary equations for determining the  $s_i$  and the angles  $\theta_i$ . These determining equations are also completely independent of  $\alpha, J$  and  $g$ . We have, therefore, the result that  $(s_1, s_2, \dots, s_{N-1}, \theta_1, \theta_2, \dots, \theta_N)$  are independent of the magnetic field ( $\alpha$ ), the total angular momentum  $J$  and the interaction strength  $g$ . These parameters, however, determine the overall scale  $R$  through eq.(12). In fact since  $s_N^2 = 1$ , the corresponding equation may be taken to be the determining equation for  $R$  in terms of the parameters of the Hamiltonian,

$$\frac{(R^2)^{\nu+1}}{4g\nu} \left[ 1 + \alpha^2 - \frac{J^2}{R^4 \phi^2} \right] = \sum_{j=1}^{N-1} \frac{1 - s_j \cos(\theta_{Nj})}{(1 + s_j^2 - 2s_j \cos(\theta_{Nj}))^{\nu+1}}. \quad (15)$$

Thus we have a *very general* result that the *geometry*, that is, the configuration modulo a common scale factor, or the shell structure of the equilibrium configuration is *independent* of the parameters of the Hamiltonian. The overall size of the system depends on the external magnetic field strength as well as on the total angular momentum  $J$ . (For further details on the influence of the magnetic field on the inter-shell rotation and diffusion, see ref. [15]). The shell structure, however, depends on the nature of the repulsive interaction through the parameter  $\nu$  but not its strength. The above analysis is valid even if any one of the  $s_i$  is zero, i.e., one particle being at the origin of the coordinate system, in which case we have two equations less (not more than one particle can be at the origin). Note that the statement above applies to *all the extremum configurations and is not just restricted to the local minima*. In Fig.1 we have shown the typical shell structure for the ground state of 25 particles as a function of  $J$  and  $\nu$ . It is easy to see that the shell structure, i.e., the number of particles in each shell and their relative orientation, is unchanged with  $J$  (modulo overall rotation). The shells get distorted with changes in  $\nu$ . Note that the system size has been normalised to the same value in Fig.1 for convenience in display.

The energy of the equilibrium configuration can be easily computed by noting that the auxiliary variable  $\phi$  defined in eq.(8) is related to the two-body potential energy by

$$\left( 1 + \alpha^2 - \frac{J^2}{\phi^2} \right) \phi = 2g\nu \sum_{i,j(j \neq i)} \frac{1}{(r_{ij}^2)^\nu}, \quad (16)$$

where the RHS is proportional to the potential energy due to interaction. Since the RHS and  $\phi$  are positive definite we have the condition  $(1 + \alpha^2)\phi^2 > J^2$ .

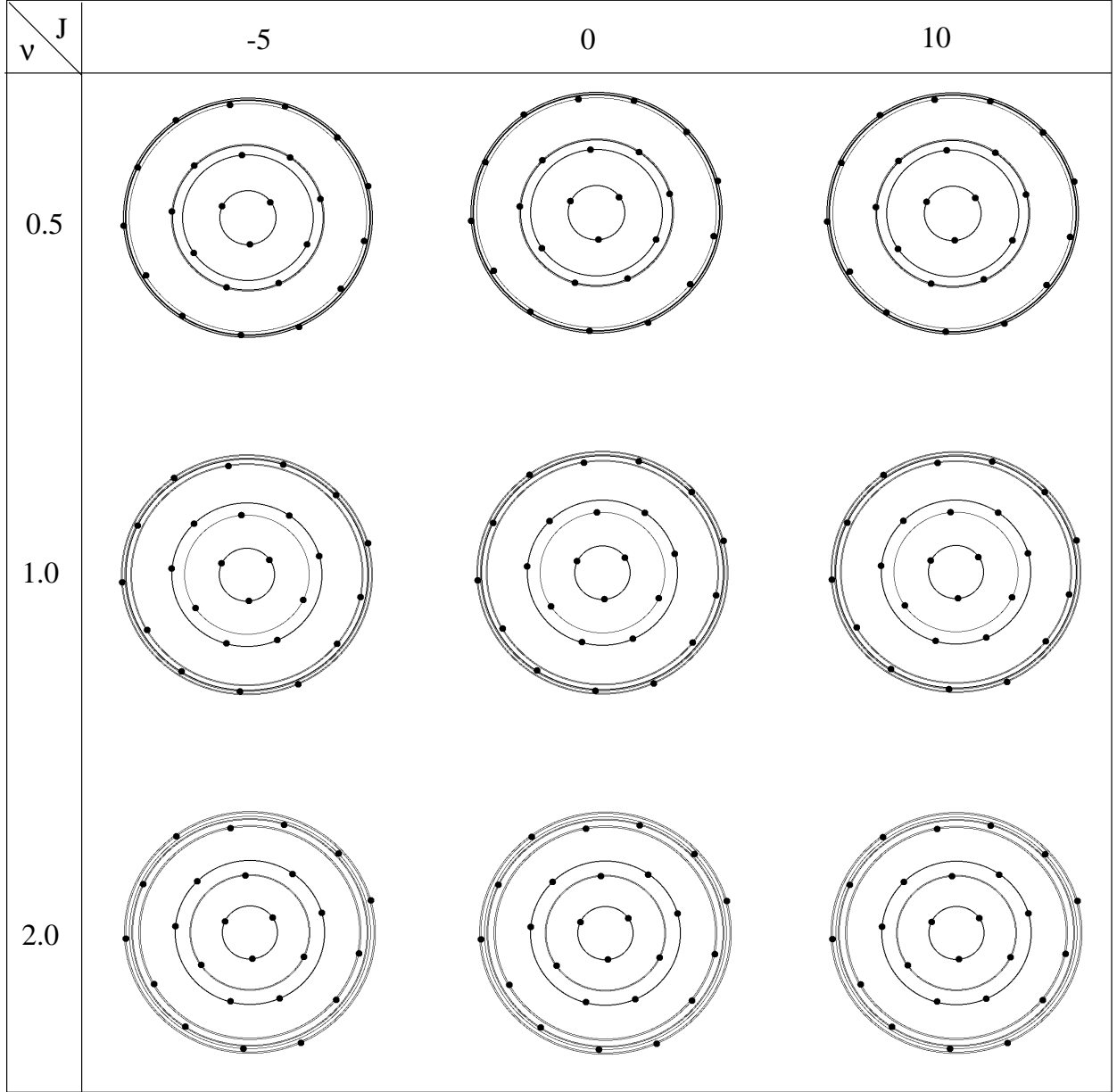


**Figure 1:** Shell structure of the ground state for 25 particles as a function of the total angular momentum  $J$  and  $\nu$ .

In the absence of the magnetic field we may set  $J = 0$  since the true ground state has zero angular momentum. In this limit, the above equation reduces to

$$\frac{1}{2} \sum_i r_i^2 = \nu \left[ g \sum_{i,j(j \neq i)} \frac{1}{(r_{ij}^2)^\nu} \right], \quad (17)$$

which implies that the confinement energy is  $\nu$  times the interaction energy. For  $\nu = 1$  both are equal, which is not surprising, since in this limit the interaction energy scales like the

kinetic energy term. We may in fact regard the above statement as a “virial” theorem valid for all equilibrium configurations.

We have, for the energy at the extrema,

$$\begin{aligned} E &= \frac{1}{2}[(1 + \alpha^2)\phi + 2\alpha J + \frac{J^2}{\phi}] + g \sum_{i,j(j \neq i)} \frac{1}{(r_{ij}^2)^\nu} \\ &= \frac{\nu + 1}{2\nu}(1 + \alpha^2)\phi + \alpha J + \frac{\nu - 1}{2\nu} \frac{J^2}{\phi}, \end{aligned} \quad (18)$$

where  $\phi = R^2 \tilde{\phi}$  and  $\tilde{\phi}$  is independent of  $J$ . This is the energy of the equilibrium configuration in a given  $J$  sector. A few comments are in order here. Consider the case when  $g = 0$ , which corresponds to the case of non-interacting confined particles in a magnetic field. This is an exactly solvable problem. From eq.(16) we have,

$$(1 + \alpha^2 - \frac{J^2}{\phi^2})\phi = 0, \quad (19)$$

which implies either (1)  $\phi = 0$  and therefore  $J = 0$  or (2)  $(1 + \alpha^2)\phi^2 = J^2$ . The first of these solutions is the trivial solution which one obtains by directly extremising the Hamiltonian. The classical solution in this case is independent of the magnetic field. The second solution, on the other hand, can be obtained only by imposing the condition of fixed  $J$  during extremisation. Equivalently, we vary the function  $F$  and not just  $H$ . The energy for a given  $J$  is then given by

$$E = \sqrt{1 + \frac{\omega_L^2}{\omega^2}} |J| + \frac{\omega_L}{\omega} J, \quad (20)$$

which is the energy of confined particles in a magnetic field. Further if we remove the confinement potential, the ground state energy is zero for all  $J \leq 0$  which is the solution for the lowest Landau level. (In the quantum mechanical case the zero point energy has to be added to the solution.). Thus the variational method in which the function  $F$  is extremised not only yields the correct energy but also the correct quantum degeneracy, which is infinite in this case.

In the general case when  $g \neq 0$ , the second step in the extremisation involves extremising the energy with respect to  $J$ , that is  $\partial E / \partial J = 0$ ,

$$\begin{aligned} &\left[ (\nu + 1)(1 + \alpha^2)R - (\nu - 1) \frac{J^2}{\tilde{\phi}^2 R^3} \right] \frac{\partial R}{\partial J} \\ &+ \frac{\nu \alpha}{\tilde{\phi}} + (\nu - 1) \frac{J}{\tilde{\phi}^2 R^2} = 0, \end{aligned} \quad (21)$$

since  $R$  depends on  $J$ . Differentiating  $R$  w.r.t.  $J$  in eq.(15) and cancelling the overall powers of  $R$ , we have

$$\left[ (\nu + 1)(1 + \alpha^2)R - (\nu - 1) \frac{J^2}{\tilde{\phi}^2 R^3} \right] \frac{\partial R}{\partial J} = \frac{J}{\tilde{\phi}^2 R^2}. \quad (22)$$



Eliminating the derivative term in the above equations, we get the following solutions at equilibrium for each configuration:

$$J = -\alpha\tilde{\phi}R^2; \quad E = \frac{\nu+1}{2\nu}\tilde{\phi}R^2. \quad (23)$$

Substituting for  $J$  in eq.(15), we get

$$R^2 = [4g\nu A(\nu, N)]^{\frac{1}{\nu+1}}, \quad (24)$$

where

$$A(\nu, N) \equiv \sum_{j=1}^{N-1} \frac{1 - s_j \cos(\theta_{Nj})}{(1 + s_j^2 - 2s_j \cos(\theta_{Nj}))^{\nu+1}}. \quad (25)$$

An important point to note here is that this energy  $E$  is *independent* of the magnetic field and its dependence on  $g$  is explicit. The dependence on  $N$  and  $\nu$  is, however, involved. The angular momentum  $J$  extremising the energy depends on the magnetic field and is zero in the absence of the magnetic field as it should be. The expressions given thus far, though, are valid independent of the geometry of the clusters and are exact (for approximate solutions see eqs.(8,9) in ref. [8] for the special case of Coulomb interaction).

We now specialise the general results given above to specific configurations which also happen to be ground states (global minima) for some  $N$ . While the results that we obtain are completely analytical and exact, the choice of configurations is based on the earlier numerical work [9]. We have also checked the veracity of these results independently using numerical methods as outlined in Appendix B.

The geometry of the clusters (or shells) is dependent on  $\tilde{\phi}$  and  $A(\nu, N)$ , which are as yet unspecified. The equations for the equilibrium configurations admit many solutions for a given  $N$  and  $\nu$ . In particular, there are two special configurations which are always solutions, viz (i) all the  $N$  particles are on a circle,  $\bigcirc$  and (ii)  $N - 1$  particles are on the circle with one particle at the center,  $\odot$ . For these two cases, only the overall scale factor  $R$  is to be determined. The angles  $\theta_{ij}/2$  are simply multiples of  $\pi/N$  and  $\pi/(N - 1)$  respectively. These configurations, however, need not be local minima in general. In particular, it has been numerically proved that for  $N \leq 5$  the circle configuration is indeed the global minimum energy configuration (ground state) whereas for  $6 \leq N \leq 8$  it is the circle-dot which is the ground state in the case of Coulomb interaction ( $\nu = 1/2$ ). The ground state exhibits multiple shell formation for  $N \geq 9$ . In what follows we prove analytically that the first transition which occurs for  $N$  from 5 to 6 is independent of  $\nu$ . However, both  $\bigcirc$  and  $\odot$  remain ground states for  $N = 5$  and  $N = 6$  respectively only for  $\nu$  up to a  $\nu_{min}$ . In Fig.2, we display the eigenvalues of the Hessian (matrix of second derivatives) of the effective potential (see eq(B.1)) as a function of  $\nu$ . When  $N = 5$ , the eigenvalues are positive definite up to  $\nu = 2.4$  for both  $\bigcirc$  and  $\odot$  configurations. Both these configurations therefore correspond to local minima, but the calculation of the energy shows clearly that the  $\bigcirc$  has lower energy and is in fact the ground state, confirming the earlier numerical calculations with  $\nu = 1/2$ . When  $N = 6$ , the eigenvalues are positive all the way up to  $\nu = 10$  (modulo a zero eigenvalue related to the rotational invariance) for the  $\odot$  configuration. Hence it is a local minimum. However the  $\bigcirc$  configuration ceases to be a local minimum for  $\nu > 0.484$  and becomes a

saddle point since one of the eigenvalues becomes negative. It is possible that there are other configurations, other than the ones considered here, which are also local minima. They are not relevant to the analysis that is to follow.

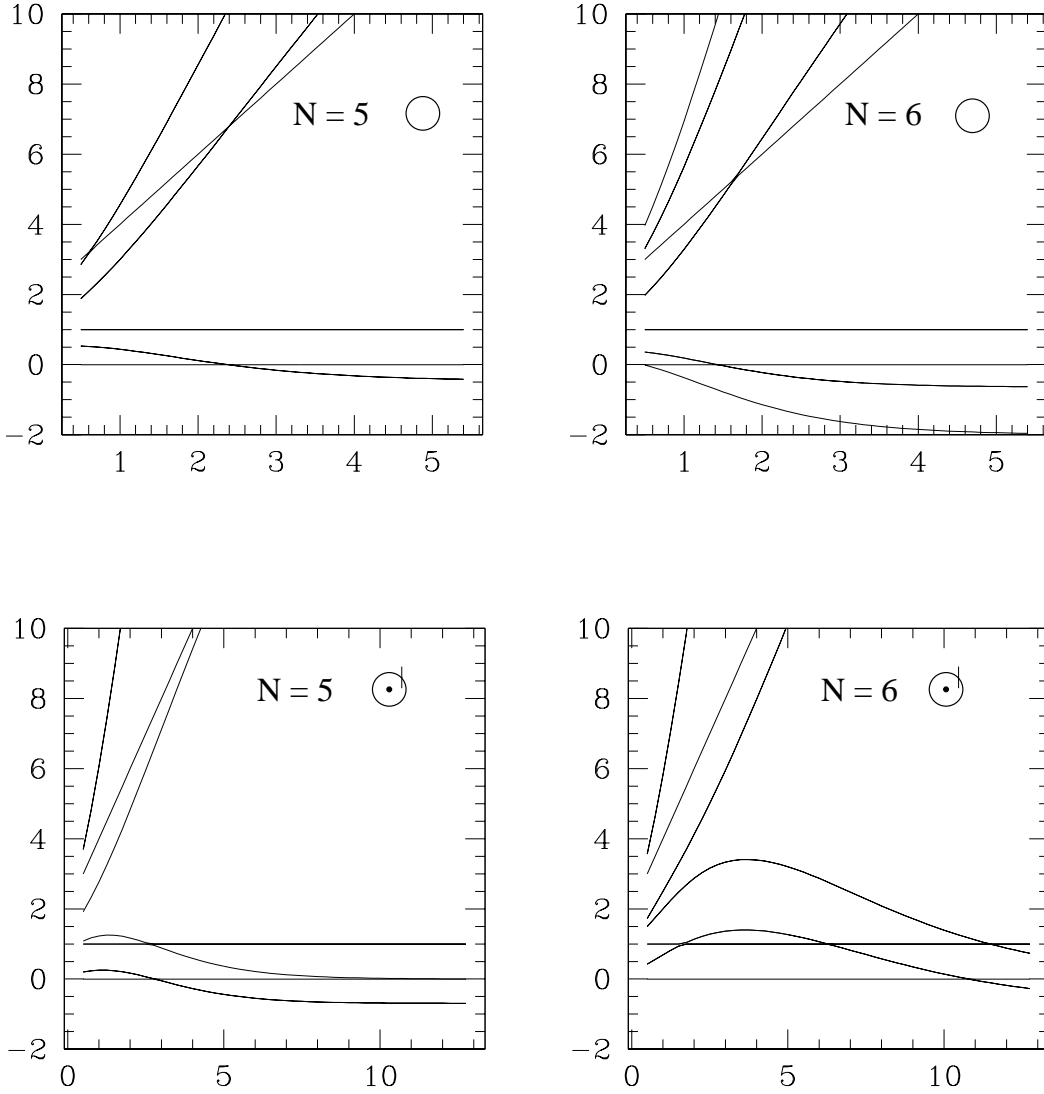


**Figure 2:** Eigenvalues of the Hessian of the effective potential as a function of  $\nu$  for  $\bigcirc$  and  $\odot$  configurations and for  $N = 5, 6$ . Positivity of the eigenvalue indicates a local minimum.

The cases of circle and circle-dot are particularly simple since there is only one scale involved, that is, all  $s_i^2 = 1, i = 2, \dots, N$  and  $s_1^2 = 1$  for the circle and  $s_1^2 = 0$  for the circle-dot.

For the circle case, we have, for  $N$  particles,

$$\tilde{\phi} = \sum_{i=1}^{N-1} s_i^2 + 1 = N \quad (26)$$

and therefore the energy is given by

$$E_{\circlearrowleft} = \frac{\nu + 1}{2\nu} [4g\nu A_{\circlearrowleft} N^{\nu+1}]^{\frac{1}{\nu+1}}, \quad (27)$$

where

$$A_{\circlearrowleft}(\nu, N) = \frac{1}{2^{2\nu+1}} \sum_{k=1}^{N-1} \frac{1}{\sin^{2\nu}(\frac{\theta_{Nk}}{2})} = \frac{1}{2^{2\nu+1}} \sum_{k=1}^{N-1} \frac{1}{\sin^{2\nu}(\frac{k\pi}{N})}. \quad (28)$$

The second equality follows from the fact that for the symmetric configuration on the circle,  $\theta_{Nk} = 2\pi(N - k)/N$ .

In the case of circle-dot, we have, for  $N$  particles ,

$$\tilde{\phi} = N - 1 \quad (29)$$

since there are now  $N - 1$  particles on the circle and one at the centre. Therefore the energy is given by

$$E_{\circlearrowright} = \frac{\nu + 1}{2\nu} [4g\nu A_{\circlearrowright} (N - 1)^{\nu+1}]^{\frac{1}{\nu+1}}, \quad (30)$$

where

$$A_{\circlearrowright}(\nu, N) = A_{\circlearrowleft}(\nu, N - 1) + 1. \quad (31)$$

The extra 1 on the RHS is the contribution of the particle at the center.

To ascertain which of the two configurations  $\circlearrowleft$  and  $\circlearrowright$  has lower energy we look at the following ratio for the same number of particles:

$$f(\nu, N) \equiv \left( \frac{E_{\circlearrowleft}}{E_{\circlearrowright}} \right)^{\nu+1} = \left( \frac{N}{N - 1} \right)^{\nu+1} \frac{\lambda_N^{(\nu)}}{\lambda_{N-1}^{(\nu)} + 2^{2\nu+1}}, \quad (32)$$

where

$$\lambda_N^{(\nu)} \equiv \sum_{k=1}^{N-1} \frac{1}{\sin^{2\nu}(\frac{k\pi}{N})}. \quad (33)$$

Note that in general the ratio  $f$  depends only on  $N$  and  $\nu$  but not on the other parameters of the model Hamiltonian. Obviously the circle is a lower energy configuration iff  $f < 1$ . We claim that, for all  $\nu > 0$ ,

$$\begin{aligned} f(\nu, N) &< 1 && \text{for } N \leq 5; \\ f(\nu, N) &> 1 && \text{for } N \geq 6. \end{aligned} \quad (34)$$

Further the function  $f(\nu, N)$  crosses unity exactly once for  $N$  between 5 and 6 and nowhere else. In Fig.3, we show the numerical values of the function  $f(\nu, N)$  as a function of  $N$  for various values of  $\nu$ .

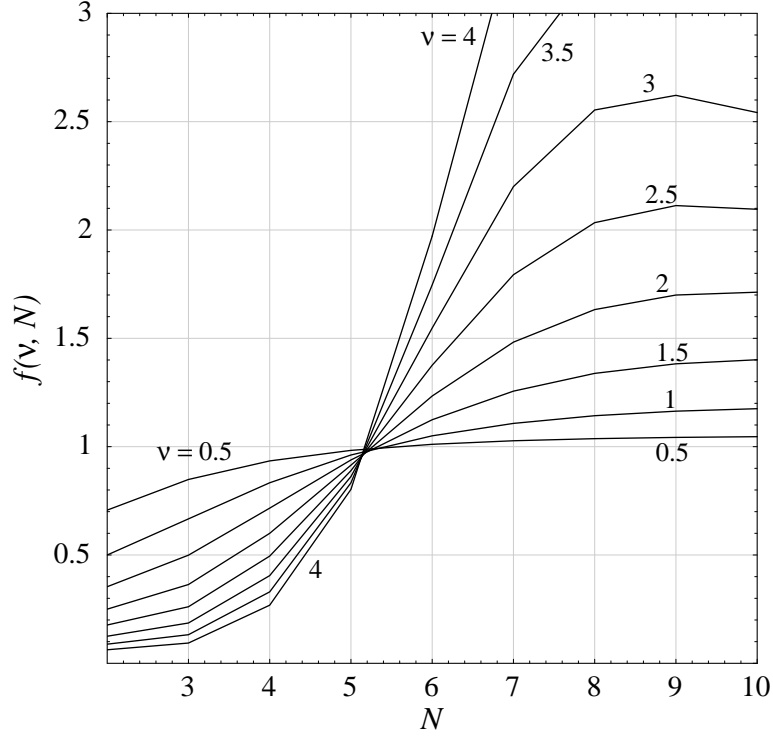


**Figure 3:** The geometric transition:  $f(\nu, N)$  vs  $N$  for  $\nu = 0.5$  to  $\nu = 4$

The result can be easily checked for  $\nu = 1$  since in this case  $\lambda_N^{(1)} = (N^2 - 1)/3$ . Therefore,

$$f(1, N) = \frac{N^2(N+1)}{(N-1)(N^2 - 2N + 24)}, \quad (35)$$

which reproduces the claims made above, for  $\nu = 1$ . For  $\nu \ll 1$ , again the proof is straightforward and we include it here since it will be relevant to the case of logarithmic interaction later. For very small  $\nu$  we make use of the identity that for any  $a$ ,  $a^\nu \approx 1 + \nu \log(a)$ . Using this identity  $\lambda_N$  may be written as,

$$\lambda_N^{(\nu)} \approx \sum_{k=1}^{N-1} (1 - 2\nu \log(\sin(k\pi/N))) = N - 1 - 2\nu X_N, \quad (36)$$

where

$$X_N = \log \left[ \prod_{k=1}^{N-1} \sin\left(\frac{k\pi}{N}\right) \right] = \log \left[ \frac{N}{2^{N-1}} \right]. \quad (37)$$

Here we have used the identity,  $\prod_{k=1}^{N-1} \sin\left(\frac{k\pi}{N}\right) = \frac{N}{2^{N-1}}$ . Further we also approximate  $(N/N - 1)^{\nu+1} \approx (N/N - 1)(1 + \nu \log(N/N - 1))$ . Substituting for  $\lambda_N$  in  $f$ , we have

$$f(\nu, N) \approx 1 + \frac{\nu}{N(N-1)} \mu_N, \quad (38)$$

where

$$\mu_N = [N(N - 3) \log(N) - (N - 1)(N - 2) \log(N - 1)] \quad (39)$$

is independent of  $\nu$ . Clearly, whether  $f$  is less than or greater than unity depends on whether  $\mu_N$  is negative or positive. However the properties of  $\mu_N$  cannot be dependent on  $\nu$ . It is now easy to see that  $\mu_N$  is negative for  $N \leq 5$  and positive otherwise. Hence the proof.

Therefore, for  $N \geq 6$ , the ground state must have multi-shell structure (including possibly  $\odot$ ). Note that the ratio  $f > 1$  or  $f < 1$  says nothing about whether the  $\circ$  or  $\odot$  is the ground state, or even local minimum. What it does say is that, if  $f > 1$ , then  $\circ$  *can not be the ground state*, independent of its stability properties. Therefore, whatever be the ground state it must have at least two shells (with one shell possibly trivial as in  $\odot$ ). This statement is independent of  $\nu$ . Thus we conclude that the first geometric transition is independent of  $\nu, g$  and  $J$ . Independent of the calculation of  $f$ , we know from numerical calculations that  $\circ$  is the ground state for  $2 \leq N \leq 5$  and  $\odot$  is the ground state for  $6 \leq N \leq 8$  for  $\nu < \nu_{max}$  where  $\nu_{max}$  is determined from the eigenvalues of the Hessian.

One could have also arrived at the conclusion that for  $N = 6$  multi-shells must form, by studying the eigenvalues of the Hessian. This however is harder to compute analytically and also is not conclusive for small values of  $\nu$  for which  $\circ$  is still a local minimum. The criterion in terms of  $f > 1$  is, however, easy and conclusive.

It therefore appears that the organisation of many-body clusters in two dimensions into shells is a robust phenomenon, independent of the nature of the repulsive two-body interaction and also independent of the Hamiltonian parameters but dependent only on the number of particles in the cluster. In particular, the first geometric transition for the ground state from circle to circle-dot configuration occurs after  $N = 5$ . The robustness of this transition seems to emerge purely from the number theoretic properties of the ratio of the energies in these two configurations. The results of this section are, however, restricted to parabolic confinement. In the next section, we analyse the effect of confinement on the geometry of clusters.

### III. EFFECT OF CONFINEMENT

While the parabolic confinement is a simple and popular choice for model systems, real systems may be more complicated. In this section, we consider a generalisation of the form of the confinement potential and study its effects on the cluster properties. For our study we choose a form of the confinement potential proposed by Partoens and Peeters [16] who have studied the influence of the form of the confinement potential and the interaction potential using numerical methods as well as an approximate Thomson model. To keep the analysis simple we do not include the magnetic field. The Hamiltonian in dimensionless units may be written as

$$H = \sum_{i=1}^N \left[ \frac{\vec{p}_i^2}{2} + \frac{g'}{2} (r_i^2)^\gamma \right] + g \sum_{i,j(j \neq i)} \frac{1}{(r_{ij}^2)^\nu}, \quad (40)$$

where  $\gamma$  characterises the confinement potential. While  $\gamma = 1$  corresponds to parabolic potential, we keep it arbitrary. The variational equations for extrema of  $F$  defined in equation (4) are straightforward to write. As before, one can eliminate the Lagrange multiplier in

favour of  $J$  and  $\phi$  (defined in eq.(8)). The equilibrium configurations are then determined by,

$$p_{ix} = -\frac{J}{\phi} y_i \quad (41)$$

$$p_{iy} = \frac{J}{\phi} x_i \quad (42)$$

$$\left( g' \gamma (r_i^2)^{\gamma-1} - \frac{J^2}{\phi^2} \right) \vec{r}_i = 4g\nu \sum_{j(j \neq i)} \frac{\vec{r}_{ij}}{(r_{ij}^2)^{\nu+1}}. \quad (43)$$

Taking the cross product in eq.(43) with  $\vec{r}_i$  gives  $N$  equations which are exactly the same as before in Section II. Taking the dot product with  $\vec{r}_i$  and dividing by  $r_i^2$ , however, gives the LHS which is *dependent* on the index  $i$ . Thus the parabolic confinement is special in this regard, since for  $\gamma = 1$  the LHS is independent of  $i$ . This fact was crucial for the conclusion that the shell structure does not depend on the total angular momentum  $J$ . In the absence of the magnetic field, we may assume that the ground state has  $J = 0$ , in which case the  $i$ -dependence of the LHS may be easily eliminated as in Sec.I. The following analysis is therefore true for all  $J = 0$  equilibrium configurations in general and in particular for the ground state.

Once again the shell structure is independent of the interaction strength. To see this we introduce an auxiliary variable,

$$\phi_\gamma = \sum_i (r_i^2)^\gamma. \quad (44)$$

Expressing  $\vec{r}_i = R\vec{s}_i$ ,  $R$  being a common scale factor (say the radius of the  $N^{\text{th}}$  particle), we write

$$\phi_\gamma = (R^2)^\gamma \left[ \sum_{i=1}^{N-1} (s_i^2)^\gamma + 1 \right] \equiv R^{2\gamma} \tilde{\phi}_\gamma \quad (45)$$

since  $s_N^2 = 1$  by choice, as in Sec.II. The basic equation determining the configuration space coordinates then takes the form

$$g' \gamma \frac{(R^2)^{\nu+\gamma}}{4g\nu} (s_i^2)^{\gamma-1} \vec{s}_i = \sum_{j(j \neq i)} \frac{\vec{s}_{ij}}{(s_{ij}^2)^{\nu+1}}. \quad (46)$$

Taking the scalar product with  $\vec{s}_i$  and dividing both sides by  $(s_i^2)^\gamma$  ( $\neq 0$ ), we get

$$g' \gamma \frac{(R^2)^{\nu+\gamma}}{4g\nu} = \sum_{j(j \neq i)} \frac{1 - (s_j/s_i) \cos(\theta_{ij})}{s_i^{2(\gamma-1)} (s_i^2 + s_j^2 - 2s_i s_j \cos(\theta_{ij}))^{\nu+1}}. \quad (47)$$

Note that the LHS is independent of the particle index  $i$  and the RHS is different from the parabolic case. However, we still have  $N - 1$  independent equations of the type

$$\begin{aligned} & \sum_{j(j \neq i)} \frac{1 - (s_j/s_i) \cos(\theta_{ij})}{s_i^{2(\gamma-1)} (s_i^2 + s_j^2 - 2s_i s_j \cos(\theta_{ij}))^{\nu+1}} \\ &= \sum_{j \neq k} \frac{1 - (s_j/s_k) \cos(\theta_{kj})}{s_k^{2(\gamma-1)} (s_k^2 + s_j^2 - 2s_k s_j \cos(\theta_{kj}))^{\nu+1}}, \quad \forall \quad k \neq i. \end{aligned} \quad (48)$$

Further by taking the cross product with  $\vec{s}_i$  and dividing by  $s_i$ , we get,

$$\sum_{j(j \neq i)} \frac{s_j \sin(\theta_{ij})}{(s_i^2 + s_j^2 - 2s_i s_j \cos(\theta_{ij}))^{\nu+1}} = 0, \quad (49)$$

which is independent of  $\gamma$  and therefore is identical to the parabolic case. This equation provides a further set of  $N$  conditions on the internal coordinates  $\vec{s}_i$ . Together eqs.(48,49) provide the  $2N - 1$  necessary equations for determining the  $s_i$  and the angles  $\theta_i$  and are completely independent of  $g$  and  $g'$ .

These, the strengths of confinement and interaction potentials, determine the overall scale  $R$  through eq.(47). Setting  $i = N$  in eq.(47), we get

$$g' \gamma \frac{(R^2)^{\nu+\gamma}}{4g\nu} = \sum_{j=1}^{N-1} \frac{1 - s_j \cos(\theta_{Nj})}{(1 + s_j^2 - 2s_j \cos(\theta_{Nj}))^{\nu+1}} \quad (50)$$

Thus we have the result that the *geometry* or the shell structure of the equilibrium configuration is *independent* of the parameters of the Hamiltonian, which only restrict the overall size of the system.

Next we compute the energy of the equilibrium configurations. To this end we note that the auxiliary variable  $\phi_\gamma$  defined in eq.(44) is related to the two-body potential energy by,

$$g' \gamma \phi_\gamma = 2g\nu \sum_{i,j(j \neq i)} \frac{1}{(r_{ij}^2)^\nu}, \quad (51)$$

where the RHS is proportional to the potential energy due to interaction. Therefore,

$$\gamma [g' \frac{1}{2} \sum_i (r_i^2)^\gamma] = \nu [g \sum_{i,j(j \neq i)} \frac{1}{(r_{ij}^2)^\nu}], \quad (52)$$

which implies that the  $\gamma$  times the confinement energy is  $\nu$  times the interaction energy. This is the generalised ‘‘virial theorem’’ valid for arbitrary confinement. We have, for the energy at the extrema,

$$E = \frac{\nu + \gamma}{2\nu} g' \phi_\gamma. \quad (53)$$

This expression for energy is valid for all equilibrium configurations. The scale  $R$  may be calculated from eq.(50) and is given by

$$R^2 = \left[ \frac{4g\nu}{g' \gamma} A(\nu, N) \right]^{\frac{1}{\nu+\gamma}}, \quad (54)$$

where

$$A(\nu, N) \equiv \sum_{j=1}^{N-1} \frac{1 - s_j \cos(\theta_{Nj})}{(1 + s_j^2 - 2s_j \cos(\theta_{Nj}))^{\nu+1}}. \quad (55)$$

and is independent of  $\gamma$ . This definition of  $A(\nu, N)$  is the same as in the parabolic case.

We now consider the effect of confinement on the geometric transition for  $N$  from 5 to 6. As shown in the previous section for parabolic confinement, the configuration changes from circle to circle-dot independent of  $\nu$ . We first give expressions for the energy for these two configurations for any  $N$ .

For the circle case, we have, for  $N$  particles,

$$\tilde{\phi}_\gamma = \left[ \sum_{i=1}^{N-1} s_i^{2\gamma} + 1 \right] = N \quad (56)$$

and therefore the energy is given by

$$E_\circ = \frac{\nu + \gamma}{2\nu} g' \left[ \frac{4g\nu}{g'\gamma} A_\circ N^{\frac{\nu+\gamma}{\gamma}} \right]^{\frac{\gamma}{\nu+\gamma}}, \quad (57)$$

where  $A_\circ(\nu, N)$  is given in eq.(28).

In the case of circle-dot, we have, for  $N$  particles,

$$\tilde{\phi}_\gamma = N - 1 \quad (58)$$

since there are now  $N - 1$  particles on the circle and one at the centre. Therefore the energy is given by

$$E_{\odot} = \frac{\nu + \gamma}{2\nu} g' \left[ \frac{4g\nu}{g'\gamma} A_{\odot} (N - 1)^{\frac{\nu+\gamma}{\gamma}} \right]^{\frac{\gamma}{\nu+\gamma}}, \quad (59)$$

where

$$A_{\odot}(\nu, N) = A_\circ(\nu, N - 1) + 1 \quad (60)$$

as before.

To ascertain which of these two configurations  $\circ$  and  $\odot$  has lower energy we look at the ratio for the same number of particles,  $N$ ,

$$\begin{aligned} f(\gamma, \nu, N) &\equiv \left( \frac{E_\circ}{E_{\odot}} \right)^{\frac{\nu+\gamma}{\gamma}} = \left( \frac{N}{N-1} \right)^{\frac{\nu+\gamma}{\gamma}} \frac{\lambda_N^{(\nu)}}{\lambda_{N-1}^{(\nu)} + 2^{2\nu+1}} \\ &= \left( \frac{N}{N-1} \right)^{\frac{\nu(1-\gamma)}{\gamma}} f(1, \nu, N) \end{aligned} \quad (61)$$

where  $\lambda_N^{(\nu)}$  is given in eq.(33) in the previous section. The effect of the confinement is therefore entirely contained in the prefactor whose exponent contains  $\gamma$ .



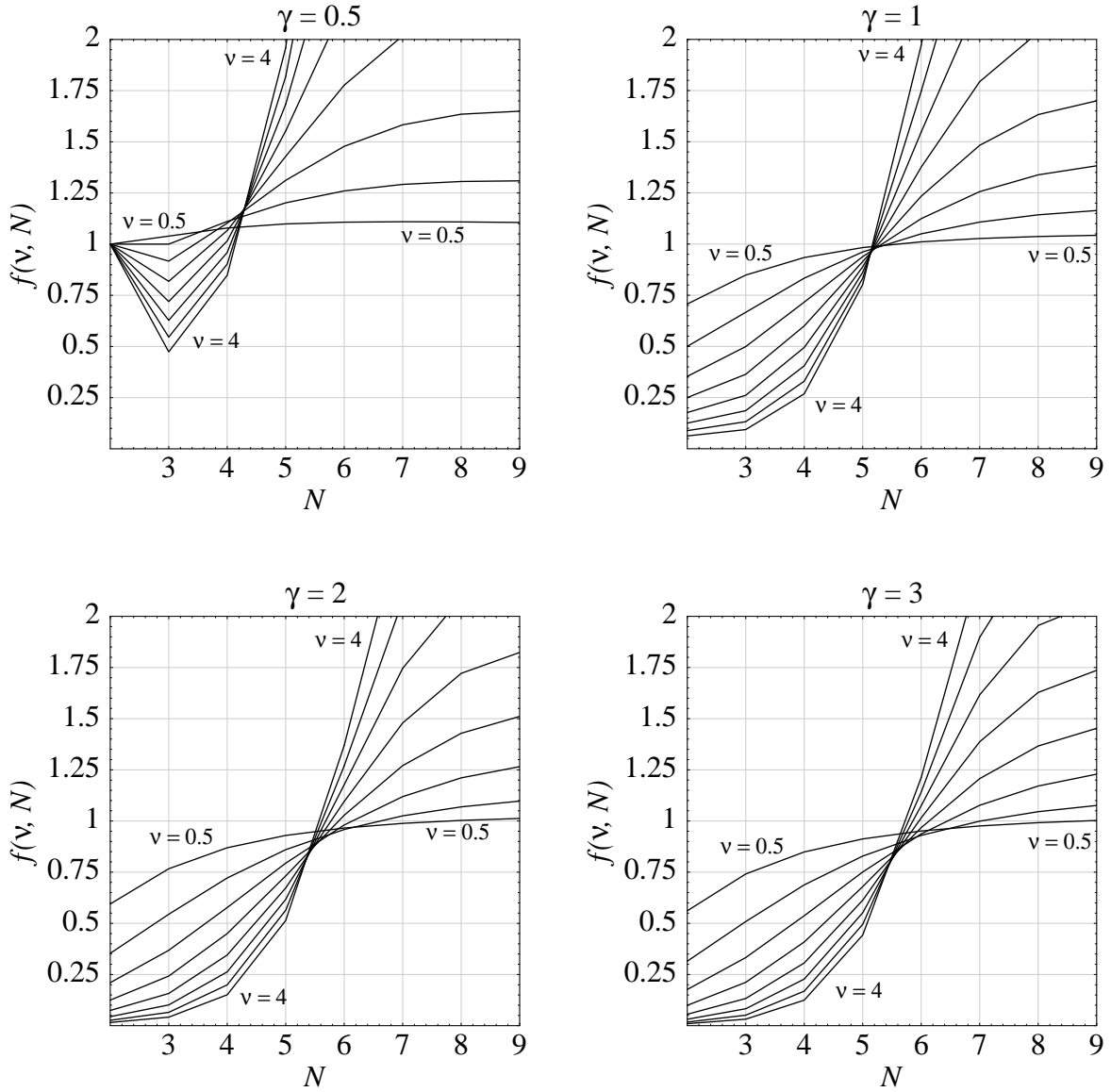


**Figure 4:** Effect of Confinement:  $f(\gamma, \nu, N)$  vs  $N$  for different values of  $\gamma$ .  
The values of  $\nu$  range from 0.5 to 4 as in Fig. 3.

In Fig.4, we show the behaviour of  $f$  as a function of  $N$  for typical values of  $\nu$  and  $\gamma$ . The pattern seen in Fig.4 may be summarised in two parts:

1. For  $\gamma < 1$ , the first geometric transition occurs before  $N = 5$ . As  $\nu$  increases the transition moves towards  $N = 5$  but never beyond. In fact there exists  $\nu_{min}$  after which the transition always occurs between 4 and 5 for  $N$ .
2. For  $\gamma > 1$ , the first geometric transition occurs after  $N = 6$ . As  $\nu$  increases the transition moves towards  $N = 5$ . For  $\nu > \nu_{min}$  the transition always occurs between 5 and 6 for  $N$ .

In the case of Coulomb interaction it was already known that the transition occurs either

before  $N = 5$  ( $\gamma < 1$ ) or after  $N = 6$  ( $\gamma > 1$ ) [16]. However the fact that the transition always occurs around  $N = 5$  after some  $\nu_{min}$  is, to our knowledge, a new result.

#### IV. EFFECT OF THREE-BODY PERTURBATIONS

In this section we consider a model Hamiltonian with a three-body interaction. While classically three-body interactions are not naturally introduced, quantum correlations can of course introduce effective many-body terms. The primary motivation for considering the three-body term here is to see if the shell structure survives under this perturbation. The effect of the three-body term is interesting and non-trivial on the first geometric transitions. The model Hamiltonian, in dimensionless units, is given by

$$H = \sum_{i=1}^N \left[ \frac{\vec{p}_i^2}{2} + \frac{1}{2}r_i^2 \right] + \frac{g_1}{2} \sum_{i,j(j \neq i)} \frac{1}{r_{ij}^2} + \frac{g_2}{2} \sum_{i,j,k(i \neq j \neq k)} \frac{\vec{r}_{ij} \cdot \vec{r}_{ik}}{r_{ij}^2 r_{ik}^2}, \quad (62)$$

where  $g_1$  and  $g_2$  are in general kept arbitrary. Notice that when  $g_2 = 0$ , this reduces to the model Hamiltonian analysed in section II with  $\nu = 1$ . The quantum mechanics with this model Hamiltonian ( $g_2 = 0$ ) has some interesting applications to quantum dots and is considered in detail in ref. [13]. The model Hamiltonian given above has a very interesting limit. When  $g_1 = g_2 = g^2$ , the quantum mechanical ground state and an infinite tower of states may be solved for exactly [17,18]. Solving the Schroedinger equation,  $H\psi_0 = E_0\psi_0$ , for the ground state we obtain

$$\psi_0 = \prod_{i < j} |r_{ij}|^g \exp\left(-\frac{1}{2} \sum_i r_i^2\right), \quad (63)$$

and the ground state energy is given by

$$E_0 = N + \frac{1}{2}gN(N-1). \quad (64)$$

In what follows we keep  $g_1$  and  $g_2$  arbitrary and comment on the case  $g_1 = g_2$  later.

The classical analysis of the model Hamiltonian is done as before by extremising the Hamiltonian in the full phase space. As in the previous section we concentrate only on the case where the total angular momentum,  $J = 0$ , which implies that  $\vec{p}_i = 0$  and the equilibrium configurations are obtained as solutions of the equations

$$\vec{r}_i = 2g_1 \sum_{j(j \neq i)} \frac{\vec{r}_{ij}}{r_{ij}^4} - g_2 \sum_{j,k(j \neq k \neq i)} \left[ \frac{\vec{r}_{jk}}{r_{jk}^2 r_{ik}^2} + \frac{\vec{r}_{ik}}{r_{ik}^2 r_{ij}^2} \right] + 2g_2 \sum_{j,k(j \neq k \neq i)} \left[ \frac{\vec{r}_{jk} \cdot \vec{r}_{ik}}{r_{jk}^2 r_{ik}^4} \vec{r}_{ik} + \frac{\vec{r}_{ik} \cdot \vec{r}_{ij}}{r_{ik}^2 r_{ij}^4} \vec{r}_{ij} \right]. \quad (65)$$

Again these equilibrium configurations may be local minima/maxima or saddle points.

The general analysis of these equations proceeds as in section II. Since there are two coupling constants  $g_1$  and  $g_2$ , the shell structure does depend on these parameters, unlike in the earlier models, except in the special case when the two are equal. Taking the dot product on both sides of the above equation with  $\vec{r}_i$  and summing over the index  $i$ , we get,

$$\sum_{i=1}^N \frac{1}{2}r_i^2 = \frac{g_1}{2} \sum_{i,j(j \neq i)} \frac{1}{r_{ij}^2} + \frac{g_2}{2} \sum_{i \neq j \neq k} \frac{\vec{r}_{ij} \cdot \vec{r}_{ik}}{r_{ij}^2 r_{ik}^2}. \quad (66)$$

Therefore the confinement energy is again equal to the interaction energy including the two- and three-body terms. Using this, the energy in any equilibrium configuration may be calculated:

$$E = \phi = R^2 \sum_{i=1}^N s_i^2 = R^2 \tilde{\phi}, \quad (67)$$

where  $s_i$  are internal variables and  $R$  is the overall scale, which may be taken to be the distance of the farthest particle from the origin. We now specialise to specific configurations namely the circle and the circle-dot. It may be easily checked that these configurations are allowed equilibrium configurations for all  $N$ . These, however, need not be local minima for all  $N$ . For these two cases, only the overall scale factor  $R$  is to be determined. The angles  $\theta_{ij}/2$ , as before, are simply multiples of  $\pi/N$  and  $\pi/(N-1)$  respectively.

For the circle case, we have, for  $N$  particles,

$$\tilde{\phi} = \left[ \sum_{i=1}^{N-1} s_i^2 + 1 \right] = N \quad (68)$$

and therefore the energy, after some algebra, is given by

$$E_{\circlearrowleft} = NR^2 = N \sqrt{\frac{(N-1)}{12} [g_1(N+1) + 2g_2(N-2)]} \quad (69)$$

In the case of circle-dot, we have, for  $N$  particles,

$$\tilde{\phi} = N - 1 \quad (70)$$

since there are now  $N-1$  particles on the circle and one at the centre. Therefore the energy is given by

$$E_{\odot} = (N-1)R^2 = (N-1) \sqrt{g_1 \left( \frac{N(N-2)}{12} + 2 \right) + g_2 \left( \frac{(N-2)(N-3)}{6} + (N-3) \right)}. \quad (71)$$

Interestingly, in the limit  $g_1 = g_2 = g^2$ , we have the important result

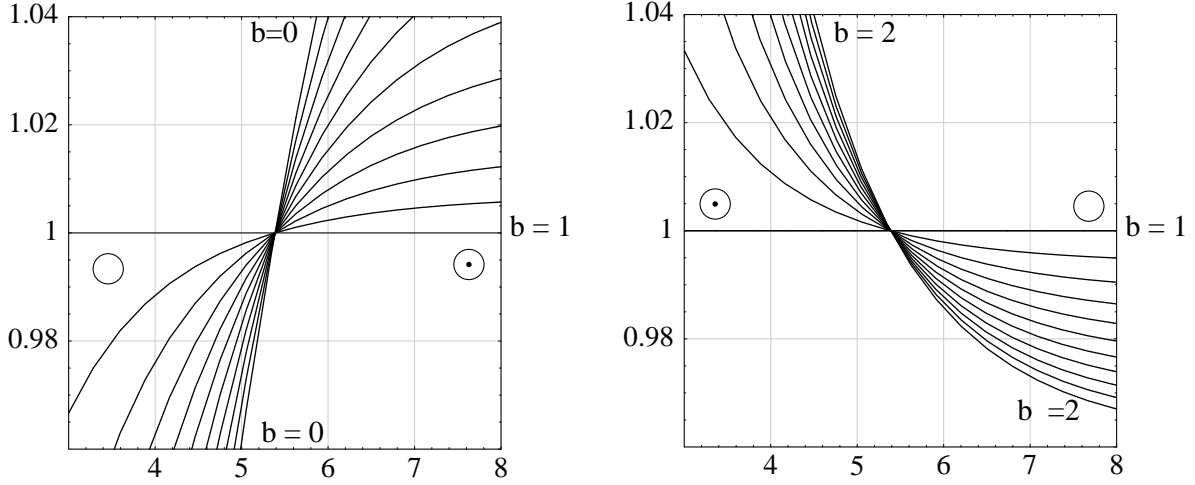
$$E_{\circlearrowleft} = E_{\odot} = \frac{1}{2} g N(N-1), \quad (72)$$

which is the same as the quantum mechanical ground state energy without the zero point fluctuation. The two configurations are also degenerate in this limit. We may therefore use either of these two classical configurations as a starting point for calculating the quantum corrections. Since the quadratic fluctuations reproduce the zero point energy the higher order corrections must be either vanishing or spurious.

Coming back to the general case,  $g_1 \neq g_2$ , we would like to examine the effect of three-body terms in the interaction on the first geometric transition from circle to circle-dot configuration. Note that in the absence of the three-body terms, circle is the ground state up to 5 particles and circle dot is the ground state for  $N=6$ . To ascertain which of these two configurations  $\circlearrowleft$  and  $\odot$  has lower energy in the presence of the three-body perturbations, it is sufficient to look at the ratio of the energies for the same number of particles:

$$f(N) \equiv \left( \frac{E_{\circ}}{E_{\odot}} \right)^2 = \left( \frac{N}{N-1} \right)^2 \frac{N^2[N+1+2b(N-2)]}{(N-1)[N(N-2)+24+2b(N-3)(N+4)]}. \quad (73)$$

where  $b$  is the ratio  $g_2/g_1$  of the strengths of the two terms. Obviously the circle is a lower energy configuration iff  $f < 1$ .



(a)  $b < 1$  (b)  $b > 1$   
**Figure 5:**  $f(N)$  vs  $N$  for various values of the ratio of the three-body to two-body strength,  $b = g_2/g_1$ . In (a)  $b$  varies from 0 to 1 in steps of 0.1 and in (b)  $b$  varies from 1 to 2 in steps of 0.1.

In Fig. 5, we show the numerical values of  $f(N)$  as a function of  $N$  for various values of  $b = g_2/g_1$ . Some interesting facts emerge from Fig. 5. First, at  $b = 1$ , the ratio is 1 since the two configurations are degenerate in this limit. For  $b < 1$ , circle has lower energy for  $N \leq 5$  and therefore  $f < 1$ . The ratio crosses unity when  $N$  changes from 5 to 6 at exactly the same point no matter what the value of  $b$  is. It is as if the three-body perturbation has no effect on this geometric transition. The energies of course explicitly depend on the coupling constants. However, for  $b > 1$ , circle has higher energy for  $N \leq 5$  and therefore  $f > 1$ . Again the ratio crosses unity between 5 and 6 and for all  $N > 6$ , circle configuration has lower energy. This can be seen analytically also, from eq.(73).

However, it turns out neither the circle nor the circle-dot configuration can be the ground state when  $b > 1$ , that is when the three-body term dominates the two-body term in the Hamiltonian. In fact the ground state is one when all particles on a line, where the particle positions are determined by the zeros of the Hermite polynomial of order  $N$  [20]. We must, however, point out that the above results are specific to the form of the Hamiltonian. Whether three-body interactions, in general, have a similar effect is a difficult question to answer.

## V. DISCUSSION

To summarise, we have discussed the shell structure of particle clusters in the presence of external confinement. To begin with, we have assumed harmonic confinement and the interaction is two-body. Following the analysis in section II, it appears that the organisation of many-body clusters in two dimensions into shells is a robust phenomenon, independent of the nature of the repulsive two-body interaction and also independent of the Hamiltonian parameters but dependent only on the number of particles in the cluster. In particular, the first geometric transition for the ground state from circle to circle-dot configuration occurs after  $N = 5$ . The robustness of this transition seems to emerge purely from the number theoretic properties of the ratios of the energies in these two configurations. A different type of confinement may in fact destroy the robustness of this transition for small  $\nu$ . The interesting point, however, is that after some critical  $\nu_{max}$ , once again the results look similar to that of the parabolic confinement.

Further, the presence of three-body terms in the interaction does not seem to affect the geometric transition as long as it remains a weak perturbation. Interestingly enough, within the model Hamiltonian we have analysed, there exists a critical point when the geometric transition changes dramatically as the perturbation strength is varied. Most importantly, the classical energy is the same as the quantum mechanical energy (without the zero point fluctuations) in the limit when the strengths of the two- and three-body terms are equal. It would be interesting to check if this is true of other many-body models where the quantum ground state is exactly known.

While the existence of the shell structure is numerically well established, the analytical understanding of the existence of the shells is lacking. It would be interesting to know how many distinct extremal configurations there are. While the first transition seems to indicate the formation of shells, a deeper understanding of the Mendeleev table is clearly called for. It would also be interesting to study quantum corrections using these classical configurations as a starting point. Such a study would be of relevance to systems in which quantum corrections are non-negligible, as in, say, quantum dot systems. Some of the aforementioned questions are being probed further.

## ACKNOWLEDGMENTS

We thank R. Balasubramanian and D. Surya Ramana for help with number theoretic identities. We thank P.P. Divakaran for pointing out the reference to Myer's work. We also thank A.P. Balachandran, Avinash Khare, Madan Rao and Surajit Sengupta for many helpful discussions.

## Appendix A: Logarithmic Interactions

We briefly discuss the case of logarithmic interaction potential with harmonic confinement in this appendix. In some quasi-two-dimensional systems like quantum dots, this may be closer to the physical situation than the power-law interactions. Specifically the Hamiltonian, in scaled units, may be written as

$$\frac{H}{\hbar\omega} = \sum_{i=1}^N \left[ \frac{\vec{p}_i^2}{2} + \frac{\vec{r}_i^2}{2} \right] - g \sum_{i,j(j \neq i)} \log \left( \frac{r_{ij}^2}{\rho^2} \right), \quad (\text{A.1})$$

where  $\rho$  is an arbitrary length parameter chosen such that  $\rho^2 > r_{ij}^2 \ \forall \ i, j$ . This is to ensure that the interaction potential is repulsive for all distances in the cluster. For simplicity, we do not include magnetic field here, though the analysis of Sec. I goes through identically in this case also. The conditions for the equilibrium are given by

$$\vec{r}_i = 4g \sum_{j(j \neq i)} \frac{\vec{r}_{ij}}{r_{ij}^2}. \quad (\text{A.2})$$

Again, by setting  $\phi = R^2[\sum_{i=1}^{N-1} s_i^2 + 1] \equiv R^2\tilde{\phi}$ , it is easy to demonstrate that the shell structure is independent of  $g$  (and also of the magnetic field, when included) as in Sec. I of the paper. Note that the equation above is manifestly independent of the arbitrary scale  $\rho$  introduced in the Hamiltonian. Further simplification occurs if we note that for any equilibrium configuration the auxiliary variable,  $\phi$  is given by

$$\phi = 2gN(N-1) \quad (\text{A.3})$$

and the energy for the equilibrium configuration is given by

$$E = gN(N-1)[1 + \log(\rho^2)] - g \sum_{i,j(j \neq i)} \log(r_{ij}^2). \quad (\text{A.4})$$

We now calculate the energy for specific configurations, namely circle and the circle-dot. For the circle case, we have, for  $N$  particles distributed symmetrically,

$$E_{\bigcirc} = gN(N-1)[1 + \log(\rho^2) - \log(2gN(N-1))] + gN(N-3) \log(N). \quad (\text{A.5})$$

In the case of circle-dot, for  $N$  particles with  $N-1$  particles distributed symmetrically on the circle and one at the centre, the energy is given by

$$E_{\odot} = gN(N-1)[1 + \log(\rho^2) - \log(2gN(N-1))] + g(N-1)(N-2) \log(N-1). \quad (\text{A.6})$$

It is not possible in general to calculate these energies unless we specify the arbitrary scale  $\rho$ . However, to ascertain which of these two configurations  $\bigcirc$  and  $\odot$  has lower energy it is sufficient to look at the difference for the same number of particles, that is,

$$\Delta E = E_{\bigcirc} - E_{\odot} = g[N(N-3) \log(N) - (N-1)(N-2) \log(N-1)] = g\mu_N. \quad (\text{A.7})$$

where  $\mu_N$  is already defined in Sec. II. Clearly the circle configuration has lower (higher) energy if  $\mu_N$  is negative (positive). Note that this statement is independent of the arbitrary scale and also the interaction strength. It is now easy to see that  $\mu_N$  is negative for  $N \leq 5$  and positive otherwise. Therefore the first geometric transition from circle to circle-dot occurs when the number of particles changes from 5 to 6, as in the case of power-law potentials.

## Appendix B: Numerical Simulations

In this appendix we briefly discuss the numerical simulations carried out for multi-shell configurations. The analysis is carried out for the Hamiltonian given in Section II for parabolic confinement and may be adapted easily for other model systems discussed in Sections III and IV. Also collected are some results on the eigenvalues of the Hessian of the effective potential at the extrema. From eq.(7) it is easy to see that the same may be obtained as  $\vec{\nabla}V_{eff}(\vec{r}_i) = 0$ , where

$$V_{eff} = \frac{1}{2} \left[ (1 + \alpha^2)\phi + \frac{J^2}{\phi} \right] + g \sum_{i,j(j \neq i)} \frac{1}{r_{ij}^2}. \quad (\text{B.1})$$

The equilibrium configurations thus are obtained by *minimising*  $V_{eff}$  numerically. For this we use the version of the conjugate gradient method [19] which uses line minimisation. Since  $V_{eff}$  is positive definite and we use line minimisation, we are guaranteed to reach the extrema which are either local minima or some times saddle points but never local maxima.

For a given number of particles, we choose several initial configurations graphically and compare the energies at the local minima. We also check that a local extremum reached is actually a local minimum by computing the eigenvalues of the Hessian of  $V_{eff}$  at the extremum. We verify the ‘‘Mendeleev’’ table of Bedanov and Peeters [9] completely for the special case of Coulomb interaction, i.e. when  $\nu = 1/2$ .

The Hessian of  $V_{eff}$  can be computed easily. It turns out that of the  $2N$  eigenvalues (for  $N$  particles), four can be obtained exactly. These also provide a check on the numerically determined eigenvalues. That the numerically determined eigenvalues contain the exact eigenvalues is also verified. Since the geometry of the extrema is independent of  $J$ , this analysis is done for zero magnetic field and  $J = 0$ . At an arbitrary point in the configuration the elements of the Hessian matrix of  $V_{eff}$  are given by

$$\frac{\partial^2 V_{eff}}{\partial x_i \partial x_j} = (1 + \alpha^2)\delta_{ij} - 4g\nu \left[ \delta_{ij} \sum_{k(k \neq i)} \frac{y_{ik}^2 - (1 + 2\nu)x_{ik}^2}{(r_{ik}^2)^{\nu+2}} - (1 - \delta_{ij}) \frac{y_{ij}^2 - (1 + 2\nu)x_{ij}^2}{(r_{ij}^2)^{\nu+2}} \right] \quad (\text{B.2})$$

$$\frac{\partial^2 V_{eff}}{\partial y_i \partial y_j} = (1 + \alpha^2)\delta_{ij} - 4g\nu \left[ \delta_{ij} \sum_{k(k \neq i)} \frac{x_{ik}^2 - (1 + 2\nu)y_{ik}^2}{(r_{ik}^2)^{\nu+2}} - (1 - \delta_{ij}) \frac{x_{ij}^2 - (1 + 2\nu)y_{ij}^2}{(r_{ij}^2)^{\nu+2}} \right] \quad (\text{B.3})$$

$$\frac{\partial^2 V_{eff}}{\partial x_i \partial y_j} = \frac{\partial^2 V_{eff}}{\partial y_i \partial x_j} = 8g\nu(\nu + 1) \left[ \delta_{ij} \sum_{k(k \neq i)} \frac{y_{ik}x_{ik}}{(r_{ik}^2)^{\nu+2}} - (1 - \delta_{ij}) \frac{y_{ij}x_{ij}}{(r_{ij}^2)^{\nu+2}} \right] \quad (\text{B.4})$$

The eigenvalue equation for this matrix is

$$\begin{pmatrix} \frac{\partial^2 V_{eff}}{\partial x_i \partial x_j} & \frac{\partial^2 V_{eff}}{\partial x_i \partial y_j} \\ \frac{\partial^2 V_{eff}}{\partial y_i \partial x_j} & \frac{\partial^2 V_{eff}}{\partial y_i \partial y_j} \end{pmatrix} \begin{pmatrix} X_j \\ Y_j \end{pmatrix} = (1 + \alpha^2)\mu \begin{pmatrix} X_i \\ Y_i \end{pmatrix} \quad (\text{B.5})$$

By grouping  $(X_i, Y_i)$  as two-dimensional vectors  $\vec{R}_i$ , one can write the matrix equation conveniently as

$$\left( \frac{1 + \alpha^2}{4g\nu} \right) (1 - \mu)\vec{R}_i = \sum_{j(j \neq i)} \frac{\vec{R}_{ij}}{(r_{ij}^2)^{\nu+1}} - 2(1 + \nu) \sum_{j(j \neq i)} \frac{\vec{r}_{ij}(\vec{R}_{ij} \cdot \vec{r}_{ij})}{(r_{ij}^2)^{\nu+2}} \quad \forall \quad i = 1 \dots N. \quad (\text{B.6})$$

At the extrema,  $\vec{r}_i$  are of course solutions of the equations

$$\left(\frac{1 + \alpha^2}{4g\nu}\right) \vec{r}_i = \sum_{j(j \neq i)} \frac{\vec{r}_{ij}}{(r_{ij}^2)^{\nu+1}} \quad \forall \quad i = 1 \dots N. \quad (\text{B.7})$$

From these equations, four exact eigenvalues and eigenvectors can be deduced immediately:

1. Both the equilibrium equations and the eigenvalue equations are manifestly rotationally covariant. One therefore expects  $\mu = 0$  to be an eigenvalue with the corresponding eigenvector  $\vec{R}_i$  denoting the rotation of the  $\vec{r}_i$ . This is indeed the case. Explicitly,  $\mu = 0$  and  $\vec{R}_i = \rho \hat{k} \times \vec{r}_i \quad \forall \quad i = 1 \dots N$  solves the eigenvalue equation when  $\vec{r}_i$  satisfy the equilibrium equations. Here  $\rho$  is an arbitrary, non-zero factor since the eigenvalue equations are homogeneous.
2. If  $\vec{R}_i = \rho \vec{r}_i$  for all  $i = 1 \dots N$ , then, using the equilibrium equations, it follows that the eigenvalue equations are satisfied with  $\mu = 2(1 + \nu)$ . Thus the equilibrium configurations themselves constitute an eigenvector with an eigenvalue which depends only  $\nu$ . In particular it is common to *all extrema for every N*.
3. It is immediately obvious that if  $\vec{R}_i = \vec{a} \quad \forall \quad i$ , then the RHS of the eigenvalue equations vanishes and  $\mu = 1$  is the corresponding eigenvalue. As there are two independent choices for the two dimensional vector  $\vec{a}$ , this eigenvalue is doubly degenerate. Note that this eigenvalue is totally independent even of the equilibrium equations.

As all these eigenvalues are common to all extrema, the remaining eigenvalues must distinguish saddle points, local minima and local maxima. Apart from providing a check on numerical simulations, these should also prove useful in computing the semi-classical corrections to the classical energies.



## REFERENCES

- [1] For a recent account of these developments, see for example, T. Chakraborty (ed.), Proceedings of the Workshop on *Novel Physics in Low Dimensional Electron Systems*, (Dresden, July 27 - Aug 8, 1997) to appear in Physica E.
- [2] P. Leiderer, W. Ebner and V. B. Shikin, Surf. Sci. **113**, 405 (1992).
- [3] J. E. Hug, F. van Swol and C. F. Zukoski, Langmuir **11** 111 (1995).
- [4] C. H. Chiang and L. I, Phys. Rev. Lett. **77**, 647 (1996).
- [5] N. F. Johnson, Contemporary Physics, **36**, 377(1995).
- [6] R. Calinon, Ph. Choquard, E. Jamin and M. Navet, in *Ordering in two dimensions*, ed. S. K. Sinha (Elsevier, New York, 1980)p.317.
- [7] Yu. E. Lozovik and V. A. Mandelshtam, Phys. Lett. **A145**, 269 (1990); Phys. Lett. **A165**,469(1992).
- [8] P. A. Maksym, Phys. Rev. **B53**, 10871(1996).
- [9] V. M. Bedanov and F. M. Peeters, Phys. Rev. **B49**, 2667(1994).
- [10] F. Bolten and U. Rossler, Superlatt. and Microstruct. **13**, 140(1993).
- [11] See for example, A. Pais, "Inward Bound" (Oxford Univ. Press, 1986) p.184 and references there in.
- [12] F. C. Zhang and S. Das Sarma, Phys. Rev. **B33**, 2903(1986).
- [13] N. F. Johnson and L. Quiroga, Phys. Rev. Lett. **74**, 4277(1995); see also J. Phys. Condens. Matt. **9**, 5889 (1997) for a detailed study of inverse square interaction.
- [14] G. Date and M. V. N. Murthy, preprint imsc/97/07/32 and cond-mat/9707291.
- [15] V. A. Schweigert and F. M. Peeters, "Time dependent properties of classical artificial atoms", to appear in J. Phys. Condens. Matter (1998).
- [16] B. Partoens and F. M. Peeters, J. Phys. Condens. Matter **9** 5383 (1997).
- [17] G. Date and M. V. N. Murthy, Phys. Rev. A **48**, 105 (1993)
- [18] A. Khare and K. Ray, Phys. Lett. **A230**, 139(1997).
- [19] W. H. Press, S. A Teukolsky, W.T. Vetterling and B. P. Flannery, *Numerical Recipes in C : The Art of Scientific Computing*, (Cambridge University Press, Second Edition, 1992)
- [20] G, Date, P. K. Ghosh and M. V. N. Murthy, preprint imsc/98/02/08, cond-mat/9802302.